Edelweiss Applied Science and Technology
ISSN: 2576-8484
Vol. 8, No. 5, 578-597
2024
Publisher: Learning Gate
DOI: 10.55214/25768484.v8i5.1719

Experimental and numerical analysis of particulate matter deposition in DPF for different blends of Algae Bio diesel

Jayant Nalawade[1], Prakash Ramakrishnan[2*]
[1,2]School of Mechanical Engineering Vellore Institute of Technology, Vellore, Tamil Nadu, India – 632 014; prakash.ramakrishnan@vit.ac.in (P.R).

Abstract: The stringent emission norms have compelled to use Diesel particulate filter (DPF) to reduce particulates emission in automotive Diesel engine. The back pressure developed in the DPF due to the Particulates matter (PM) deposition in porous zone degrades the diesel engine's performance. So, there is a need of a fuel which should produce less particulates on combustion as well as its produced particulates should be easy to get regenerated inside the DPF. Three different Algae biodiesel blends B20, B40 and B60 were selected for the study, while the results are compared with the diesel fuel. A numerical study has been done with diesel and Algae biodiesel blends to investigate the effect of PM deposition on the DPF performance. The results of PM concentration and the pressure drop has been predicted for t = 2000s. and compared with the results predicted for diesel fuel. The summarized velocity contours and the PM concentration plots show that a maximum of the PM concentration was found in the diesel fuel case, while the lower found in B60 algae blend. Also, the pressure drop was found to increase with the increase in PM deposition in each case of fuel. The SEM-EDS analysis is done after collecting PM samples after combustion shows a higher percentage of Oxygen and lower Carbon with an increment of Biodiesel in the blend. This work provides a brief idea about the PM deposition in DPF while using Diesel and Algae Biodiesel blends and highlighting the better fuel option for Diesel Engine.

Keywords: *Diesel particulate filter (DPF), Energy dispersive X-ray spectroscopy (EDS), Particulate matter (PM) deposition, Particulate matter oxidation, Regeneration, Scanning electron microscopy (SEM).*

1. Introduction

There are rising concerns about the emission from automobiles due to their contrary health effects and global climate change. Diesel engines are commonly used for heavy-duty vehicles as a power source due to their low fuel consumption, reliable performance and durability [1]. Unfortunately, these vehicles can produce a considerable number of emissions which causes the air pollution. The exhaust emissions of high-power diesel vehicles include the harmful nanoparticles of carbon monoxide, nitrates, hydrocarbons NOx, and particulate matter (PM), which are detrimental for human beings [2]. PM contains a fraction of soluble organic particles and soot. Particulate matter from the exhaust of diesel engines vehicles is carcinogenic in nature, which can threaten human life [3]. Diesel Particulate Filter (DPF) is commonly measured as the most effective after-treatment device to reduce and control harmful emissions particles. At present, many emission control methods like alternative fuels and electric vehicle are used to resolve the environmental pollution problem with stringent emission standards [4]. Many studies reported that, alternative fuels such as hydrogen, ethanol and biodiesel are less emission producing fuels [5]. Bio-diesel produced from vegetable oils, animal fat, waste oil are renewable fuels and contains methyl esters of fatty acids. A life cycle analysis indicates that biodiesel can reduce up to 19% of life cycle petroleum consumption [6]. It is well-known that neat biodiesel or its blends in

* Correspondence: prakash.ramakrishnan@vit.ac.in

various percentages have a great oxygen content or higher air entrainment due to a higher boiling range [7]. Hence, bio-diesel can reduce the level of PM mass emission.

Nowadays, the DPF technology, an after-exhaust treatment technique, is an effective method for Particulate matter control to meet current and future government regulations [4]. The diesel engine furnished with DPF arrangement has lower PM, as it has the maximum filtration efficiency. However, the continuous deposition of particles inside the wall of DPF leads to the engine's poor performance due to increased engine back pressure [8]. The engine will ultimately stop its function once the back pressure extends its limit. Hence, there is a need to take action for removing the accumulated particles. The process of eliminating accumulated particles from the DPF is known as oxidation of PM or regeneration. Three different techniques *viz.* passive, active and mixed passive-active regeneration, are used to oxidize particulate matters, particularly DPF [4, 9–11]. A pre-catalyst activity can be helpful for dropping the regeneration temperature in a passive type regeneration, which further reduces the DPF regeneration time [12–14]. While in active technique, support of fuel burner or external heater was employed to enhance the inlet temperature to ~550 °C or higher. The mixed type method is relevant if the filters are catalyzed and pre-heated.

Different researchers are fascinated towards the blended fuels like biodiesel and ethanol with diesel to lessen the particles and gaseous emissions. On the other hand, many studies concentrated on the use of DPF with the Particulate matter regeneration process. Tsuneyoshi et al. [15] designed a hexagonal pore filter to decrease the emission concentration and, ultimately the backpressure in the DPF. They found higher regeneration efficiency compared with the quadrilateral pore structure. Fang et al. [16] examined the effect of operating parameters such as exhaust flow rate on the regeneration process of DPF. They concluded with the negative impact of exhaust flow rate on maximum temperature gradient and regeneration ratio without considering the oxygen content. Wu et al. [17] explored the flow characteristics of exhaust at the entry region of DPF. They found a higher deposition or gathering of Particulate matter particles at the center part of the DPF filter. Similarly, Gong et al. [18] specified a non-uniform Particulate matter particle distribution but diverges in various regions of DPF in filter substrate for both lower and higher particle concentrations. Fernandez et al. [12] verified different fuels experimentally in an assembly of Euro 5 engine and DPF. Four types of fuels *viz.* diesel, e-diesel, paraffinic and biodiesel are considered for the analysis. Results shows a better capability of Particulate matter from paraffinic and oxygenated bio-fuels lower oxidation temperature, while e-diesel Particulate matter was found less sensitive to the oxygen concentration. They also mentioned that biodiesel is more cost-effective regeneration through an active process due to its more reactive nature than the other fuel tested.

Several experimental and numerical studies have been conducted to understand the influences of different exhaust conditions on the deposition of Particulate matter in DPF. Yamamoto et al. [19] did numerical simulations on Particulate matter deposition in DPF. They used a lattice Boltzmann method to investigate the flow behavior in real DPF. A 3D X-ray method was used to scan the structure of cordierite filter. Both, Particulate matter deposition for particulate matter trap and the Particulate matter combustion were examined using numerical simulations. They concluded the flow path and change in pressure inside the cordierite filter structure were depends on the non-uniformity of the pore structure. The flow field changes significantly with Particulate matter deposition, with higher back-pressure. Further, in 2012, Yamamoto and Yamauchi [20] presented a numerical study on Particulate matter deposition and regeneration. They suggested that, the temperature of the filter was kept 800 K or higher to avoid the clogging in DPF to achieve a continuous regeneration. Ben said et al. [21] did an experimental study to investigate the Particulate matter deposition in DPF channels. A geometric analysis inside the DPF in regards with Particulate matter deposition profiles and regeneration was presented. A mathematical model was used to simulate the similar phenomenon and results were validated with the experimental results. Mahadevan et al. [22] investigated effect of temperature and PM distribution on catalyzed DPF, experimentally and numerically. A multi-zone particulate filter

Edelweiss Applied Science and Technology
ISSN: 2576-8484
Vol. 8, No. 5: 578-597, 2024
DOI: 10.55214/25768484.v8i5.1719

(MPF) model was used for the numerical analysis to examine the temperature and PM distribution inside the DPF. They validate the model with experimental results.

The above literature indicated that different researchers worked on the effect of DPF structural parameters and exhaust characteristics on the flow field, temperature field, and Particulate matter deposition rate. Also, some literature found on the use of alternative fuels such as biodiesel on the Particulate matter deposition and ultimately DPF performance. This paper aims to investigate the exhaust characteristics using different fuels (diesel and Algae bio-diesel) and their effect on the Particulate matter deposition inside the DPF. The exhaust characteristics can be found experimentally and their results were used to simulate the Particulate matter deposition phenomenon in DPF. The Particulate matter concentration and respective pressure drop were predicted numerically. The soot characterization is done using SEM-EDS to check the chemical content and morphology of PM samples.

2. Materials and Methods

2.1. Fuels and Their Properties

The exhaust characteristics of two fuels Diesel, and Algae Bio-diesel have been analyzed in experimental test. Chlorella vulgaris, green-colored eukaryotic based micro-algae is used to extract the biodiesel. Preparation of biodiesel from crude algae oil by Transesterification, it is a process of using methanol (CH_3OH) in the presence of catalyst (Potassium hydroxide KOH) to chemically break their molecule of crude algae oil into ester and glycerol. This process is a reaction of the oil with an alcohol to remove the glycerin, a by-product of biodiesel production. The different properties of the neat bio-diesel and diesel were figure out with different in-house equipment's in the lab. Table 1 explains the properties of the diesel and neat bio-diesel. Three different blends of Algae bio-diesel with different volume fraction named B20, B40 and B60 was considered for the analyses and results were compared with diesel fuel.

Table 1.
Fuel properties of the algae biodiesel and the diesel.

Property	Diesel	B20	B40	B60	B100
Calorific value (MJ/kg)	45.5	44.58	43.67	42.76	40.93
Flash point (◦ C)	52.2	69.96	87.72	105.48	141
Fire point (◦ C)	96.1	106.48	116.86	127.24	148
Cloud point (◦ C)	- 12	-10	-8	-6	-2
Pour point (◦C)	- 18	-16.6	-15.2	-13.8	-11
Density (kg/m^3)	832	857.6	883.2	908.8	960
Kinematic viscosity (m^2/s)	4.09× 10^-6	4.42× 10^-6	4.76× 10^-6	5.10× 10^-6	5.77× 10^-6
Dynamic viscosity (kg.m/s)	0.00335	0.00375	0.00422	0.00467	0.00554

2.2. Experimental Test Set Up

An experimental test has been carried out to find exhaust characteristics and pressure drop in a DPF for different fuels used in analysis. A two-cylinderAtalon vertical inline diesel enginewith a capacity of 21kW (28 bhp at 2000 rpm), connected to a 100bhp eddy current dynamometer as shown in Figure 1 was used. Different particulate matters or smoke for different samples of fuels was observed and recorded at constant engine operating conditions (1500 rpm and 100% of peak load).A mechanical Micro Bosch fuel injection pump and a multi-hole nozzle injector is used in the test bed.Incylinder pressure and its cyclic variation data was recorded by a Kistler 701A piezoelectric pressure transducer mounted on the cylinder head and the proportional crank angle was recorded using a rotatory encoder model E50S8-360-3-T-5 made by Autonics, Korea.A standard square channel DPF was used for the

Edelweiss Applied Science and Technology
ISSN: 2576-8484
Vol. 8, No. 5: 578-597, 2024
DOI: 10.55214/25768484.v8i5.1719

analysis of pressure drop. The details about the specification of the DPF used are provided in table 2. A schematic of the experimental test setup was shown in figure 1.In this research work, the pressure drop analysis for DPF with 100% loading condition for the validation of numerical results.The exhaust from the diesel engine is connected through pipe to DPF inlet. The exhaust characteristics were recorded at the inlet of the DPF. The temperature and velocity of the exhaust gas were recorded at inlet and outlet of the exhaust. The pressure drop was measured across the DPF.The parameter of combustion like knocking, heat release rate etc. was measured using the EPA 1.0.1 Engine Performance analyser software. The emission parameter such as CO_2 and CO are measured in terms of percentage volume and the unburnt NOx and HC are recorded in terms of parts per million (ppm) using an AVL 444 gas analyser based on the non-dispersive infrared (NDIR) principle for before and after the DPF. An AVL 432C smoke meter was used to measure the smoke opacity. The PM samples are collected with the help of Glass Micro Fibre filter from the exhaust of each fuel for SEM-EDS analysis.

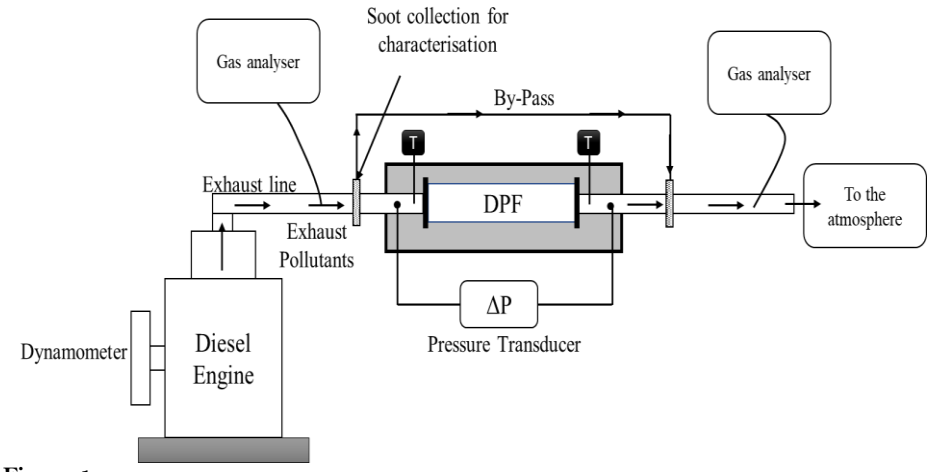

Figure 1.
Schematic of the experimental test setup.

Table 2.
technical specifications of the DPF.

Characteristics	Details
Filter diameter	140 mm
Filter length	150 mm
Wall thickness	0.40 mm
Filter density	450 kg/m^3
Thermal conductivity of DPF Substrate	1.4 W/mK

3. Numerical Methodology for Particulate Matter Deposition

A CFD-based model of Particulate matter deposition and regeneration was developed for a single-channel catalytic DPF.Figure 2shows a schematic of the two-dimensionalcomputational domain consisting of inlet channel, outlet channel and porous regions (wall of the filter and cake layer).When the engine exhaust gas flows from the inlet channel into the outlet channel through the porous filter wall, the Particulate matterincluding soluble organic matter (SOF) is trapped on the filter wall in the inlet channel, eventually the cleaned exhaust gas is discharged from the exhaust pipe into the atmosphere.

Edelweiss Applied Science and Technology
ISSN: 2576-8484
Vol. 8, No. 5: 578-597, 2024
DOI: 10.55214/25768484.v8i5.1719

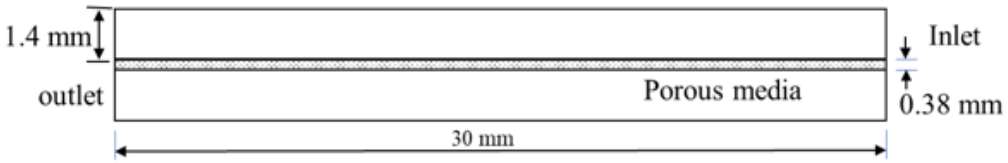

Figure 2.
Shows the computational domain for the analysis.

The 2-D single channel is considered for the DPF Exhaust gas recirculation. The Input conditions are defined by exhaust gas data obtain from the diesel engine combustion for various blends. For all cases B20, B40 and B60 blend the exhaust conditions has been analyzed experimentally, which can be used for the analysis of Particulate matter deposition and Particulate matterregeneration. Thebiodiesel is mixed with fossil-based diesel fuel with volume basis at a proportion of 20%, 40%, and 60%as per requirement. The exhaust results have been recorded for the different loading conditions of the engine (100 % loading conditions). The speed of the engine (1500 rpm) was kept constant for all the cases. Two processes are included in the simulation. One is the Particulate matter deposition for PM trap in the DPF structure using experimental results of exhaust. The other is the Particulate matter combustion to examine the filter regeneration with the catalytic effect using deposition results.

3.1. Particulate Matter Deposition Model

The DPF is basically filter, which is going to filter out the PM particle in diesel exhaust. Therefore, the simple porous media simulation is preferred. The cell zone conditions are defined according to the functions of the flow. The filtration area is considered as the porous region. The inlet flow is considered as turbulent flow, exhaust from the engine. The species model is considered for modeling the flow which is consisting of the CO_2, CO, NO_2 and O_2 with the soot. For adding the Particulate matter to the inlet mixer to DPF, Particulate matter model is selected as Soot-Moss Brook. Thevolumetric reaction is considered with thermal diffusion and Eddy-Finite rate reaction. The Reaction takes place in the DPF is Oxidation reaction with catalyst SiC.Theoxidation of the CO is takes place producing CO_2 also Particulate matter deposition is going to take place in the filter region. The Realizable K-ε Model is selected for the simulation of the turbulent flow. The pressure conditions are kept atmospheric at inlet and outlet. Soot Moss Brook model is implemented to simulate the Particulate matter in the inlet mixture Yamamoto 2009 [20]. The slow oxidation process is taking place. The Arrhenius Equation is selected to represent the oxidation reaction with pre-expiation factor and activation energy (Darcy equation).

A mass fraction of the particulate matter and smoke has been calculated from the experimental exhaust analysis report. The soot, O_2, CO_2 and CO mass fraction has been set with different conditions of the inlet fuel (Diesel and Algae bio-diesel). Velocity inlet and temperature was implemented as inlet boundary conditions. For all cases velocity of the exhaust was kept constant at 3 m/s, while a temperature is set to 700 K. Initial conditions for the DPF is set to constant for all cases. The Initial Conditions are mentioned in Table 3.

Table 3.
Initial boundary conditions

Initial conditions	Value
Temperature at the DPF	300 K
Particulate matter concentration at DPF	0 kg/m^3
Filter Porosity	0.5
Viscous Resistance at porous Media	2.00 x E^{12}

Edelweiss Applied Science and Technology
ISSN: 2576-8484
Vol. 8, No. 5: 578-597, 2024
DOI: 10.55214/25768484.v8i5.1719

3.2. Mathematical Modeling

The Particulate matter deposition model is used with the standard flow balance equations which are mentioned follow,

The Continuity equation-

$$\frac{\partial(\varepsilon\rho)}{\partial t} + \vec{\nabla}(\rho\vec{V}) = S_\rho \tag{1}$$

Where ε is the local porosity (void fraction), ρ is the fluid density, V is the velocity (in the porous regions, it is the superficial velocity),andS_ρ is the mass source term a rising as a result of the Particulate matter consumption (it only applies in the porous regions).

Momentum equations:

$$\rho u\frac{\partial u}{\partial x} + \rho v\frac{\partial u}{\partial y} = \frac{\partial}{\partial x}\left(\mu_e\frac{\partial u}{\partial x}\right) + \frac{\partial}{\partial y}\left(\mu_e\frac{\partial u}{\partial y}\right) - \frac{\partial P}{\partial x} \tag{2}$$

$$\frac{\partial(\rho uv)}{\partial x} + \frac{\partial(\rho v^2)}{\partial y} = \frac{\partial}{\partial x}\left(\mu_e\frac{\partial v}{\partial x}\right) + \frac{\partial}{\partial y}\left(\mu_e\frac{\partial v}{\partial y}\right) - \frac{\partial P}{\partial y} \tag{3}$$

Species conservation:

$$\frac{\partial(\varepsilon\rho y_i)}{\partial t} + \vec{\nabla}\left(\rho\vec{V}y_i + \vec{J_\imath}\right) = S_{yi} \tag{4}$$

Where y_i, J_i and S_{yi} are the mass fraction, diffusive mass flux and volumetric mass generation at i'th species, respectively.

3.3. Energy Conservation

It was assumed that, in the porous regions, the fluid and solid (i.e., silicon carbide – SiC – for the wall and Particulate matter for the cake layer) phases are in local thermal equilibrium. This implies that, in any control volume, the fluid and solid have the same temperature.

$$\left(\rho c_p u\right)\frac{\partial T}{\partial x} + \left(\rho c_p v\right)\frac{\partial T}{\partial y} = k\left(\frac{\partial^2 T}{\partial x^2} + \frac{\partial^2 T}{\partial y^2}\right) + \dot{S} \tag{5}$$

Particulate Matter Conservation (Porous Zones):

$$\frac{\partial m}{\partial t} = -\dot{\omega_s} \tag{6}$$

Where m is the local Particulate matter concentration [kg/m³] and ω_s is the Particulate matter reaction rate [kg/m³ s].

Particulate matter Moss Brook Equation for Particulate matter deposition in Porous media-

The Moss-Brookes model solves transport equations for normalized radical nuclei concentration and Particulate mattermass fraction:

$$\frac{\partial}{\partial t}(\rho Y_{soot}) + \nabla.(\rho\vec{v}Y_{soot}) = \nabla.\left(\frac{\mu_t}{\sigma_{soot}}\nabla Y_{soot}\right) + \frac{\partial M}{\partial t} \tag{7}$$

$$\frac{\partial}{\partial t}(\rho b_{nuc}) + \nabla.(\rho\vec{v}b_{nuc}) = \nabla.\left(\frac{\mu_t}{\sigma_{nuc}}\nabla b_{nuc}\right) + \frac{1}{N_{norm}}\frac{\partial N}{\partial t} \tag{8}$$

$$b_{nuc} = \frac{N}{\rho N_{norm}}$$

Edelweiss Applied Science and Technology
ISSN: 2576-8484
Vol. 8, No. 5: 578-597, 2024
DOI: 10.55214/25768484.v8i5.1719

Were, $Y_{soot}$is the Particulate matter mass fraction, b_{nuc} radical nuclei concentration, NParticulate matter particle number density.

To establish the accuracy of the CFD solution, and to keep the computational costs low a mesh independence study of the heat sink domain is important. Prior to performing the CFD simulations, a grid independence study was conducted over three grid resolutions. A grid independency study has been performed to set the minimum computation time required for the analysis. Hexahedral types cells were generated in structured grid. The structural mesh has aids over the unstructured type cell elements. Five different size grids have been used for similar boundary conditions to analyses soot concentration. Table 4 shows the details about the mesh with respect to their soot concentration results. An academic based ANSYS ICEM software was used for generating the mesh. Convergence criteria were set to 10^{-4} for continuity and momentum equation while 10^{-6} for energy equation. A fine grid size was used with an average skewness and orthogonal quality of 0.412 and 0.0.356, respectively with 1.52 Lac numbers of elements. It is found that, there is marginal difference between the surface temperatures with all three grid sizes.

Table 4.
Grid dependence test results with diesel fuel case.

Sr. No.	Element size	Number of elements	Soot concentration(kg/m³)
1	0.005	864230	0.8880
2	0.015	430602	0.8880
3	0.025	151308	0.8879
4	0.035	77247	0.8873
5	0.045	46903	0.8868

3.4 Validation of DPF Simulation Model

In order to ensure the accuracy of the numerical model, it is necessary to verify the results of the model with experimental test results. A pressure drop across the DPF was validated with the experimental results. The results of pressure drop from simulation and experimental test setup was shown in Figure 3. The pressure drop increases with time, as the trapped soot clogs the pores of the fibre material, reducing the void fraction. The greater the concentration of soot, the greater the pressure drop. A rather good agreement is established between the numerical data and the experimental results. Porous materials, such as fibre quartz and silicon carbide (SiC), are better suited for the monolithic catalytic filter, in which exhaust gas is driven through the porous wall.The error between the simulation model and the experimental test results is small and the path of the pressure is generally consistent with the testing values. However, the small difference in the results due to the selected DPF for experimental test setup was merely used for short time period. Hence, the test values are slightly higher than the simulated values. Hence, this model can be used to predict the pressure drop in DPF.

Edelweiss Applied Science and Technology
ISSN: 2576-8484
Vol. 8, No. 5: 578-597, 2024
DOI: 10.55214/25768484.v8i5.1719

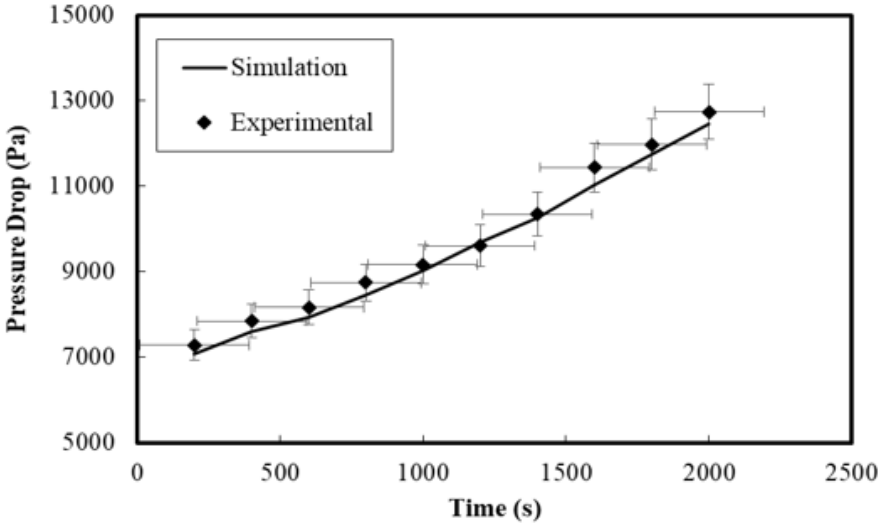

Figure 3.
Validation of the numerical model with experimental results.

4. Results

4.1. Emission Results of Diesel and Algae Bio-Diesel Blends

The emission parameter such as CO_2 and CO are measured in terms of percentage volume and the unburnt NOx and HC are recorded in terms of parts per million (ppm) using an AVL 444 gas analyser based on the non-dispersive infrared (NDIR) principle. An AVL 432C smoke meter was used to measure the smoke opacity. All the measurements were taken for 100% loading conditions and without EGR condition. The results exhaust for all fuels (diesel, B20, B40 and B60) are tabulated in Table 5. The results were used to account the inlet conditions for the numerical analysis. The Particulate matter deposition with respect to each fuel exhaust conditions were analysed in numerical analysis. The least reactive component was determined to be soot from fossil diesel fuel, as its oxidation occurred at the highest temperature levels. Due to the fact that soot particles were the incomplete products of compressed initiated combustion, they exhibited combustion characteristics and appeared later with decreasing initial temperature. The soot emissions in this case were a result of both soot production and oxidation. Under higher ambient temperature circumstances, poorer premixed combustion occurred, resulting in increased fuel richness inside the biodiesel fuel jet, increased soot formation rates during the early stages of combustion, and lastly, increased time integrated soot mass. The primary results show that, the use of Algae bio-diesel along with diesel can reduce the emissions.

Table 5.
Exhaust results for diesel and algae bio-diesel blends.

Fuel	Load	Speed	Exhaust temp	Smoke (%vol)	CO (% vol)	HC (ppm)	CO_2 (% vol)	O_2 (% vol)	NO_x (ppm)
Diesel	100%	1500	420	95	0.02	11	7.3	18.23	850
B20	100%	1500	455	86	0.02	10	6.2	12.49	860
B40	100%	1500	473	76	0.04	5	4.4	14.7	971
B60	100%	1500	480	70	0.03	5	2.2	18.32	989

4.2. PM Characterization of Algae Biodiesel Blends

The morphology of Algae Biodiesel has been characterized by a Scanning electron microscope (SEM) from the soot samples collected and the SEM images observed. The scanning electron

Edelweiss Applied Science and Technology
ISSN: 2576-8484
Vol. 8, No. 5: 578-597, 2024
DOI: 10.55214/25768484.v8i5.1719

microscopy combined with energy dispersive X-ray analysis using Zeiss EVO 50 Modal, Oxford EDS, Modal X-Max was used for the analysis. A computer operated field emission SEM equipped with an EDS detection system was used to conduct the SEM–EDS analyses. Different samples of algae bio-Diesel blends and plain diesel oil were collected on Carbon Tape & to make the samples electrically conductive; a very thin layer of Gold (Au) was deposited on the surface. The Figure 4 shows the SEM-EDS images with the inset line scan results showing the chemical compositions of those micro-scale precipitates within and along the grain boundaries of diesel and different Biodiesel blends, where the different elemental composition along with its local mass is measured with technique. SEM-EDS line scans in inset table presents in images in Figure 4 (a-c) show the results of various composition in a particular location as per the small precipitate (>10 μm) in a sample. The maximum carbon weight percentage was found 90% for the B20 blend. It is seen that, as the percentage of Algae Bio-Diesel increased into the diesel the carbon percentage will reduced and Oxygen percentage will get increased. The minimum carbon percentage was found 78.9% for B60 blend fuel.

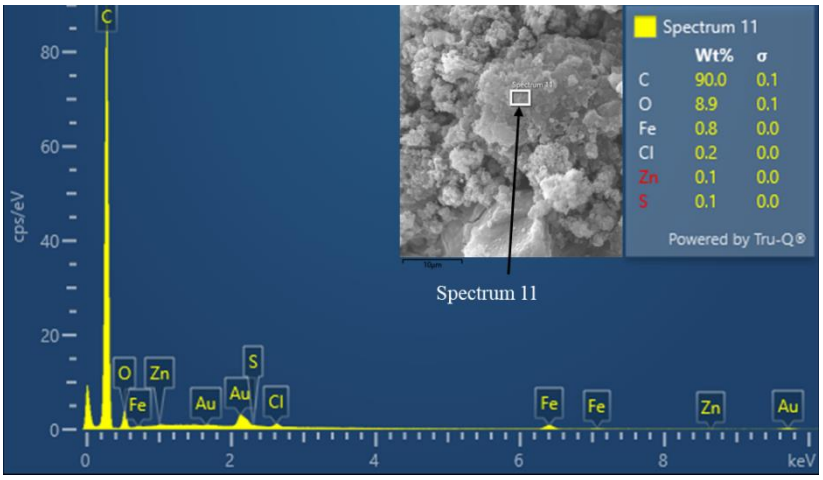

(a) SEM-EDS of B20

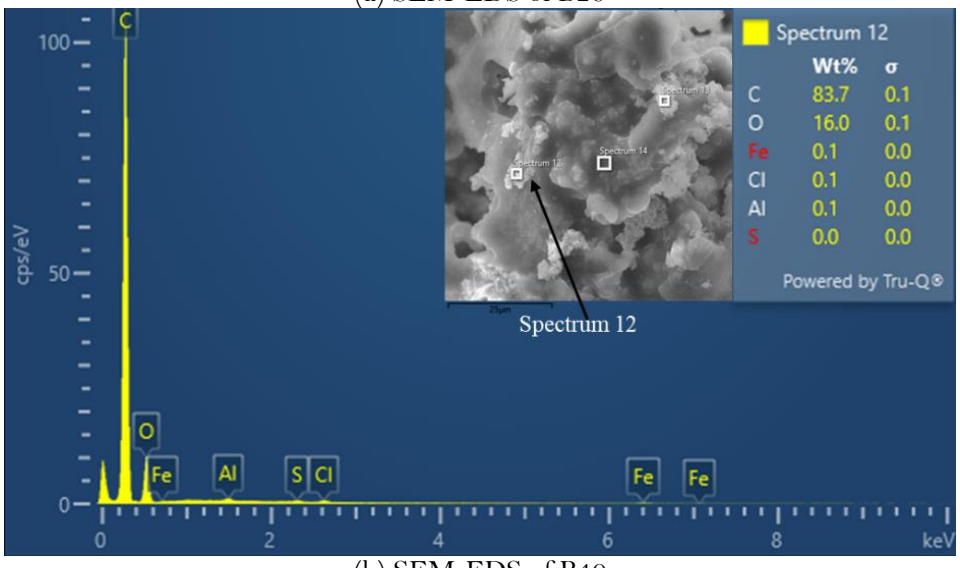

(b) SEM-EDS of B40

Edelweiss Applied Science and Technology
ISSN: 2576-8484
Vol. 8, No. 5: 578-597, 2024
DOI: 10.55214/25768484.v8i5.1719

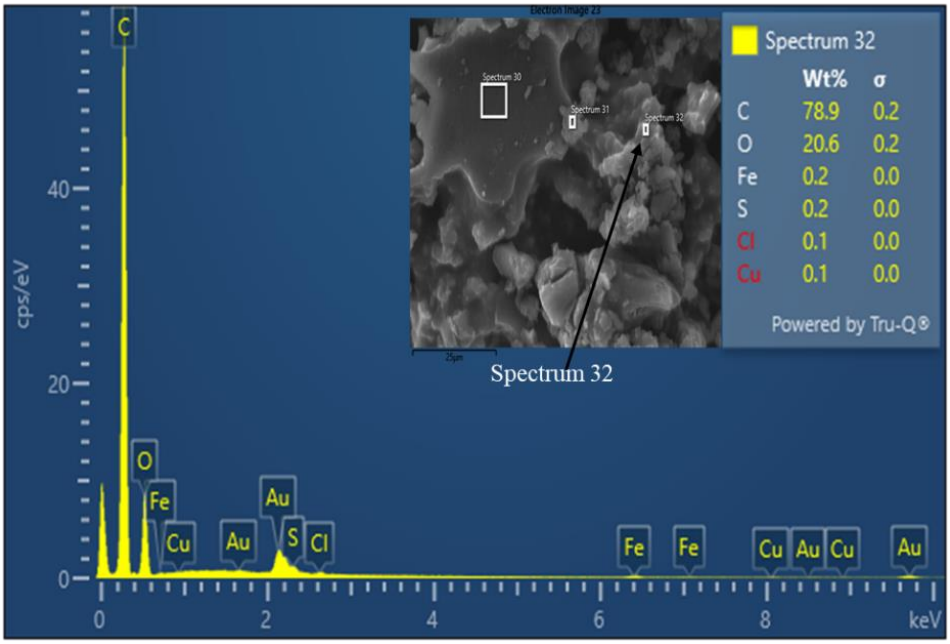

(c) SEM-EDS of B60

Figure 4.
SEM –EDSimages with the inset line scan results showing the chemical compositions of those micro-scale precipitates within and along the grain boundaries forMicroalgae Biodiesel blend fuels.

Table 6 shows the exact values of composition present in each sample of algae fuel and Diesel which shows that the maximum carbon content (90%) was found in B20 blend fuel while the B60 blend has the minimum carbon percentage (~78.9%).

Table 6.
Chemical compositions of different PM samples.

	Diesel	MA B20	MA B40	MA B60
C	90.2	90	83.7	78.9
O	8.1	8.9	16	20.6
Fe	0.8	0.8	0.1	0.2
Cl	0.3	0.2	0.1	0.1
Zn	0.4	0.1	0	0
S	0.1	0.1	0	0.2
Na	0.1	0	0	0
Ca	0.1	0	0	0
Al	0	0	0.1	0
Cu	0	0	0	0.1

Figure 5 shows the SEM-EDS Colour mapping of PM composition collected from Diesel and different biodiesel blends, where the various compositional elements are colour coded for identification. The analysis is particularly useful when we compare the different HAADF images taken from different fuel blends to recognise the compositional changequalitatively. Figure 3 (a) shows the high angle annular dark field (HAADF) image Microalgae B20 blend, also the corresponding element mapping of C, Fe, Mn, Cl, O and S are shown in Figure 5 (b). HAADF-STEM images are used to extract the information of the trace metals present in the collected soot. The different color combination in HAADF-STEM images represents a particular trace metal.Figure 5 (a) depicts that trace metals such as

Edelweiss Applied Science and Technology
ISSN: 2576-8484
Vol. 8, No. 5: 578-597, 2024
DOI: 10.55214/25768484.v8i5.1719

C, Fe, Mn, Cl, O, and S in particulate originate from the test fuels and concentration seems to be uniform distribution.The higher concentration in a specific color in figure, the higher is the presence of traces of respective metal in sample.

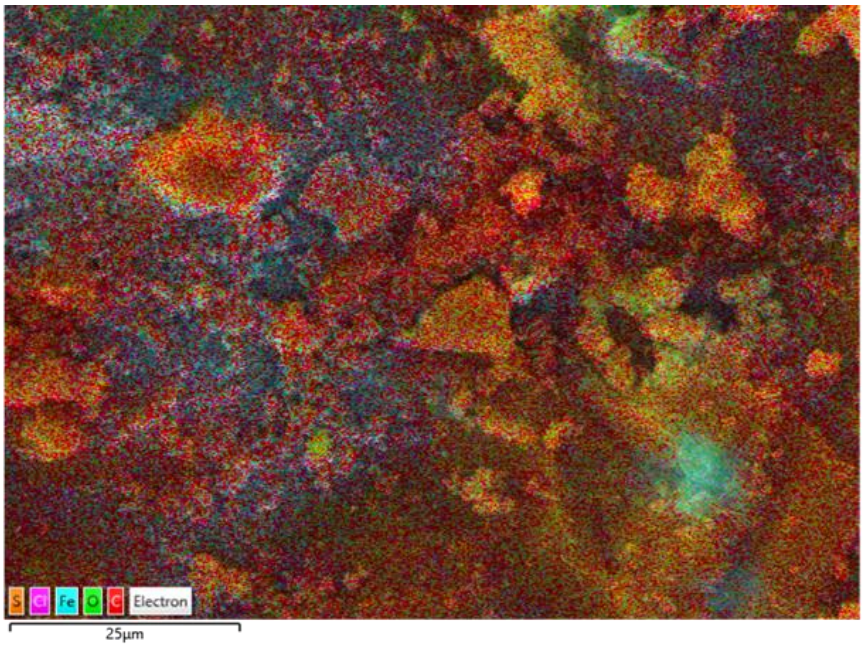

(a) High angle annular dark field (HAADF) image Microalgae B20 blend

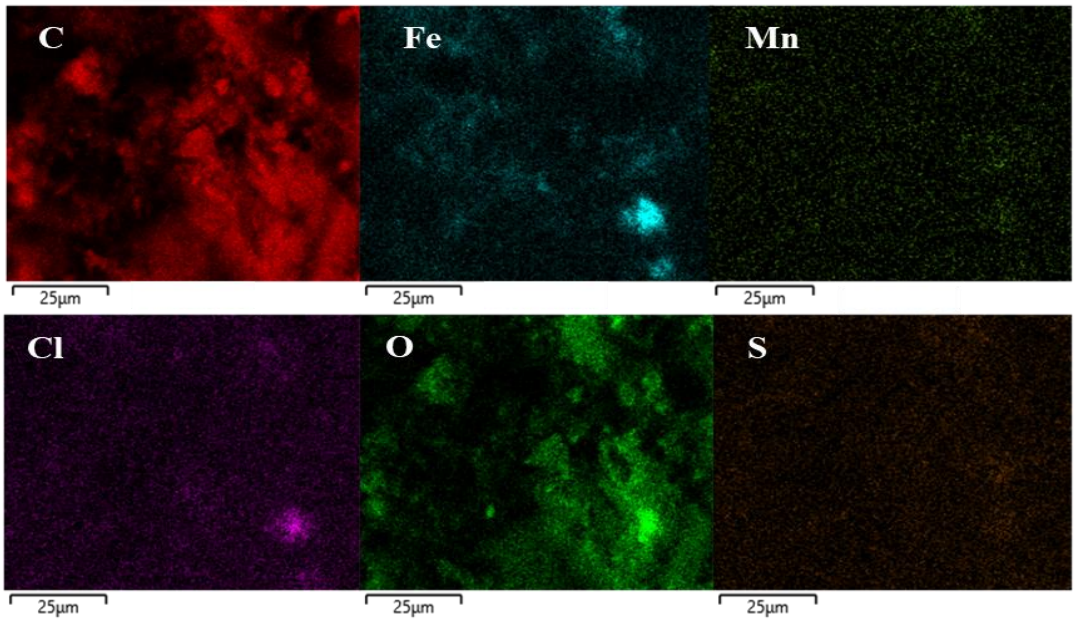

(b) High angle annular dark field (HAADF) image for corresponding elements mapping in sample.

Figure 5.
(a) High angle annular dark field (HAADF) image Microalgae B20 blend, (b) corresponding element mapping of C, Fe, Mn, Cl, O and S.

Edelweiss Applied Science and Technology
ISSN: 2576-8484
Vol. 8, No. 5: 578-597, 2024
DOI: 10.55214/25768484.v8i5.1719

Figure 6 shows PM Agglomerate structure in which a high magnification images are collected to analyse the morphology. PM agglomerates collected on Glass microfiber filter from the exhaust of different biodiesel blends & neat Diesel. The SEM image analysis gives limited information due low magnification values. The bigger agglomerates can be analyzed for its form, shape and sizes. Through this analysis it's observed that all the PM samples show powdered form and don't have any specific shape. TEM can be used for further deep insights about morphological changes in Particulate Matter.

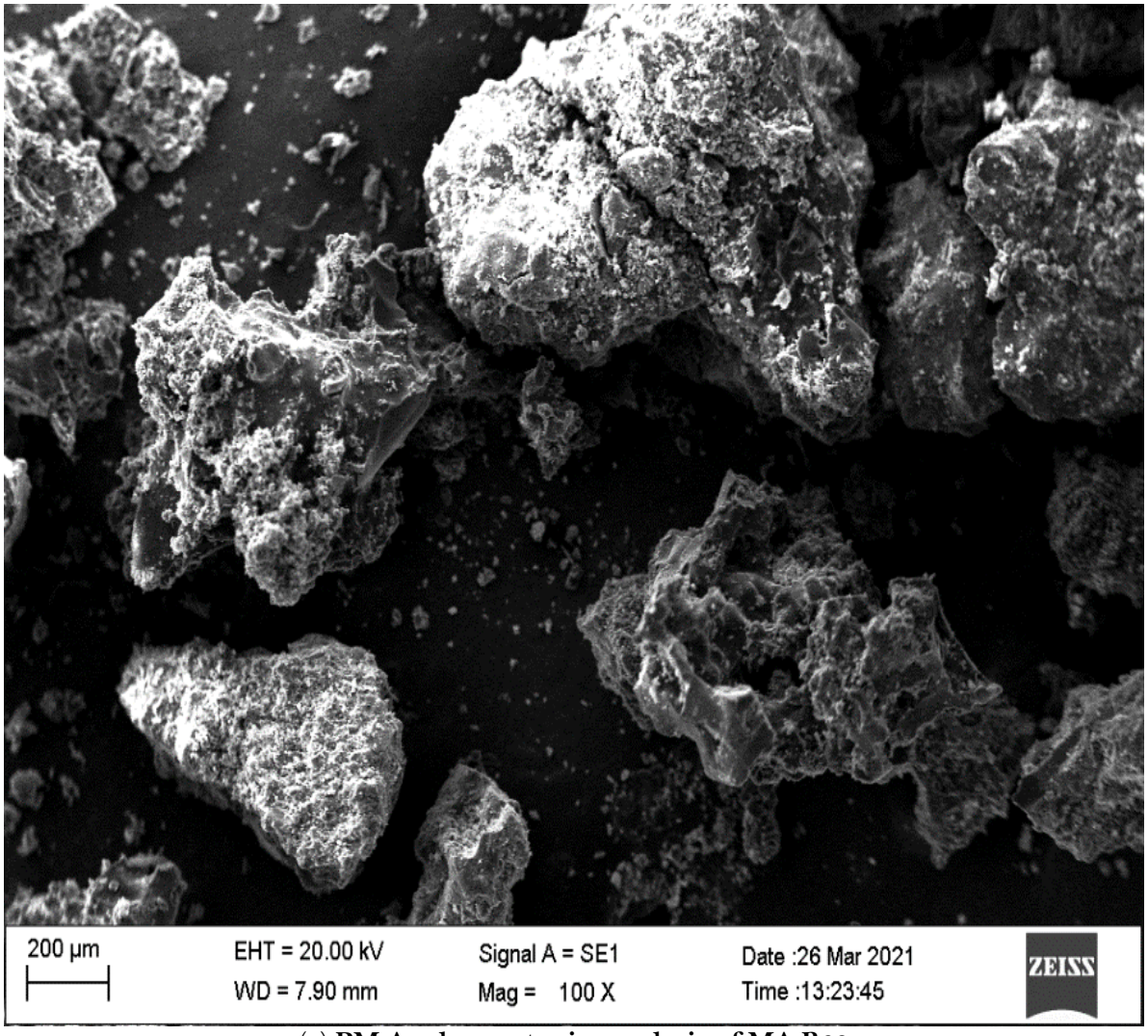

(a) **PM Agglomerate size analysis of MA B20**

Edelweiss Applied Science and Technology
ISSN: 2576-8484
Vol. 8, No. 5: 578-597, 2024
DOI: 10.55214/25768484.v8i5.1719

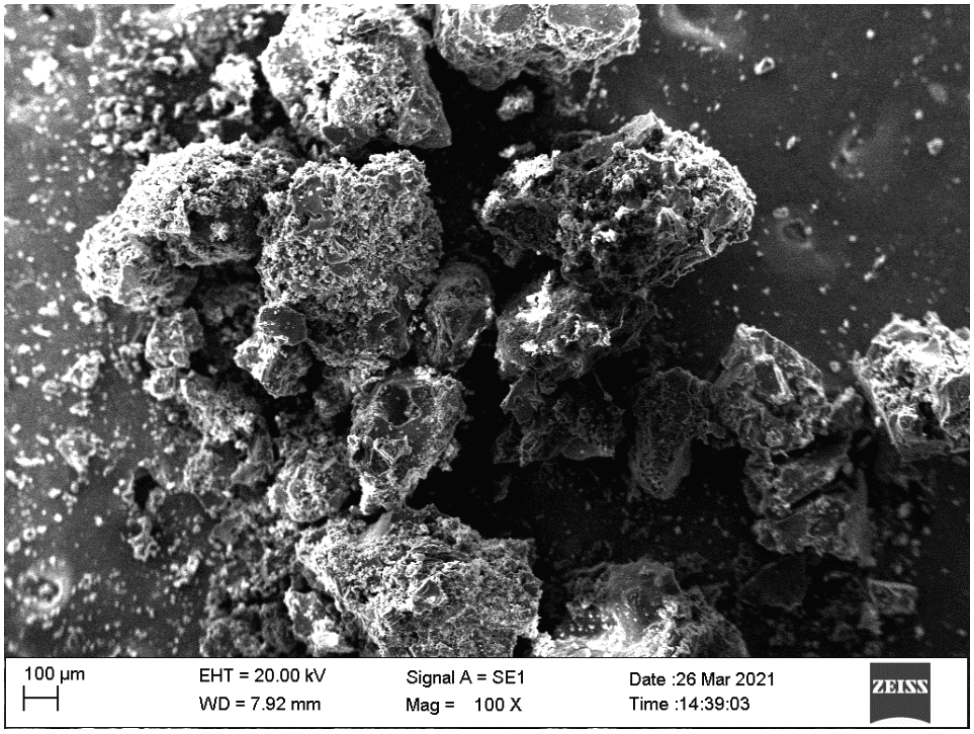

(b) **Agglomerate size analysis of MA B40**

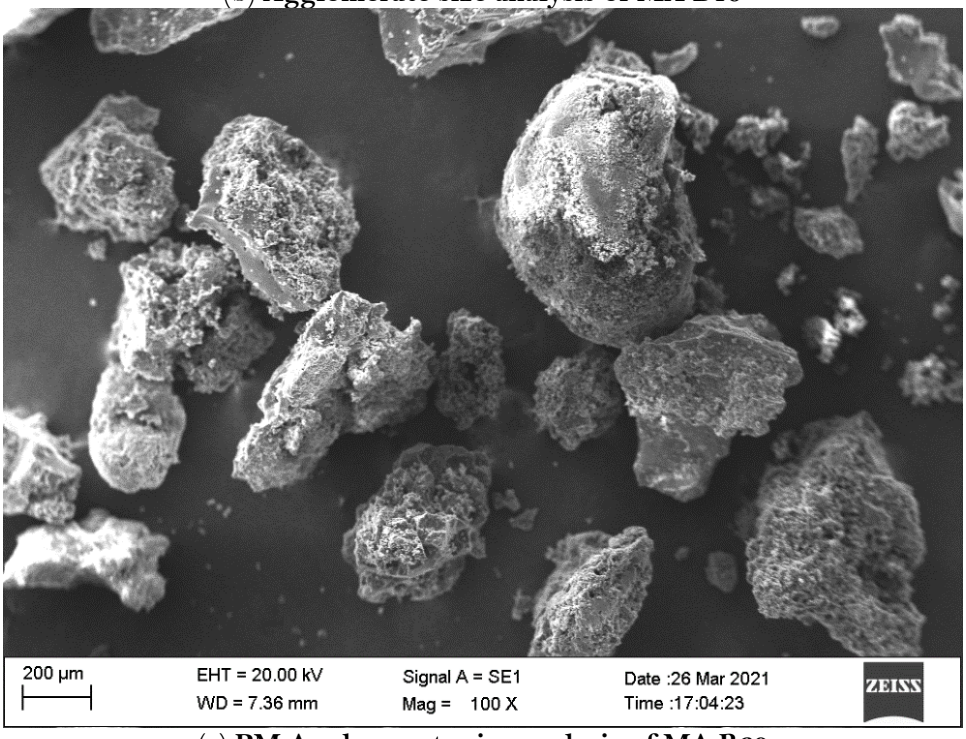

(c) **PM Agglomerate size analysis of MA B60**

Figure 6.
PM Agglomerate size analysis of Diesel and Algae Biodiesel blends.

Edelweiss Applied Science and Technology
ISSN: 2576-8484
Vol. 8, No. 5: 578-597, 2024
DOI: 10.55214/25768484.v8i5.1719

4.3. Particulate Matter Deposition in the DPF

The Particulate matter deposition for the various types of Algaeblend (B20, B40 and B60) can be analyzed numerically through ANSYS Fluent software. The results of Particulate matter concentration and the pressure drop can be predicted for 2000 sec. and compared with the results predicted for diesel fuel. Theparticulate matter concentration plots were summarized here.

Figure 7 shows the Particulate matter concentration at porous media and cake layer for different fuels for 2000 sec. From the figure it can be seen that, the Particulate matter concentration was increase with increase in time. The Particulate matter particles are flows from inlet to outlet within a porous media, Particulate matter particle are trapped at the porous media and deposited. It is observed from figure that, the diesel fuel has more Particulate matter deposition than the other fuel. The algae bio-diesel blends produces lesser Particulate matter hence the deposition was found lesser than the diesel fuel. The maximum Particulate matter deposition was found 0.8879 kg/m^3 for diesel fuel while it is found maximum of 0.7871 kg/m^3 for B20 blend. The minimum Particulate matter deposition at 2000 second was found 0.7072 kg/m^3 for B60 blend. The physical trapping of the soot particles with porous wall in the DPF can reduce the soot emissions. The use of oxygenated alternative fuels in diesel engines may result in significant improvements when it comes to DPF regeneration, as the lower temperature required results in a more efficient regeneration process (thus minimizing the fuel consumption penalty related to active regeneration). Non-oxygenated paraffinic fuels also provide advantages, but to a lesser level.Particulate Matters has been deposited onto the surface of the porous wall and the channels, which results in increasing pressure drop. Soot particles first trapped in porous filter zone hence the porosity and the permeability of the filter reduced [21, 22]. A pressure drop across the test channel was calculated for every case of fuel, and results are shown in figure 8. It can be observed that, the pressure drop increases with increase in Particulate matter concentration. The maximum pressure drop for three cases Algae bio-diesel fuel was found 12.94 kPa for B20 blend. As Particulate matter deposited into the DPF, it can resist the flow of the exhaust gases which can create the back pressure into the system. The minimum pressure drop was found 11.28 kPa for B60 blend.

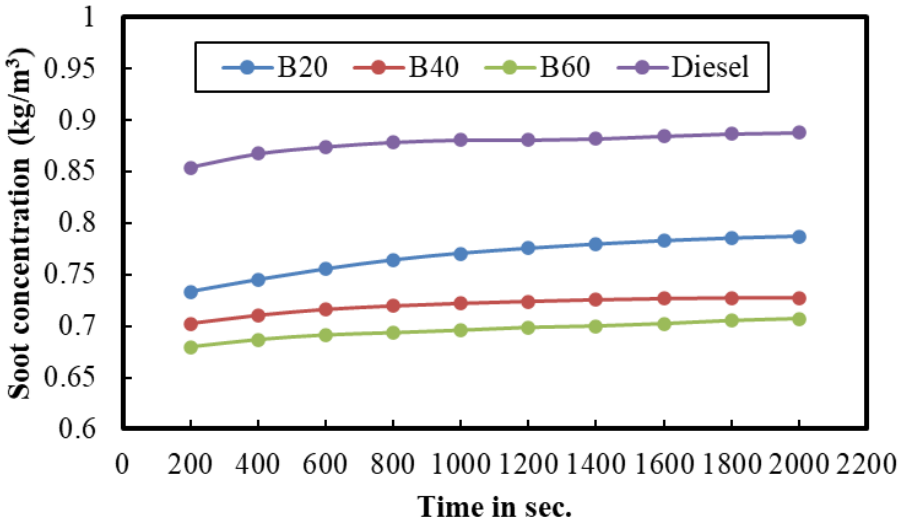

Figure 7.
Particulate matter concentration in porous media versus time in sec.

Edelweiss Applied Science and Technology
ISSN: 2576-8484
Vol. 8, No. 5: 578-597, 2024
DOI: 10.55214/25768484.v8i5.1719

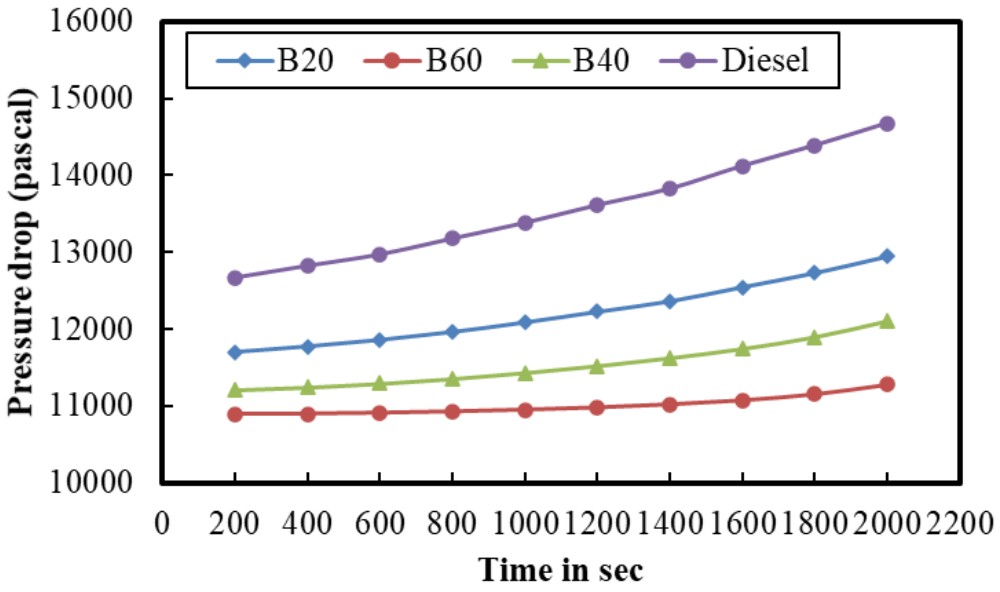

Figure 8.
Pressure drops with DPF versus time in sec.

The Particulate matter accumulation of in porous region is shown in figure 9 for different time. As explained earlier, the Particulate matter deposition at the wall of the DPF increased with the exhaust flow into the porous region. The particulate matters with different size can accumulate the porous zone with different loading conditions of engine. The maximum Particulate matter concentration has been found at 2000 sec. At the entry region, the Particulate matter concentration was less as the flow rate is higher. The flow maldistribution due to the friction and other parameters at the filter channels was significantly influenced on soot deposition, which causes the uneven soot deposition inside the DPF channels. The ignition temperature and the oxygen level also have the impact on the soot deposition [19]. A non-uniform concentration of the soot can be seen in figure 9.

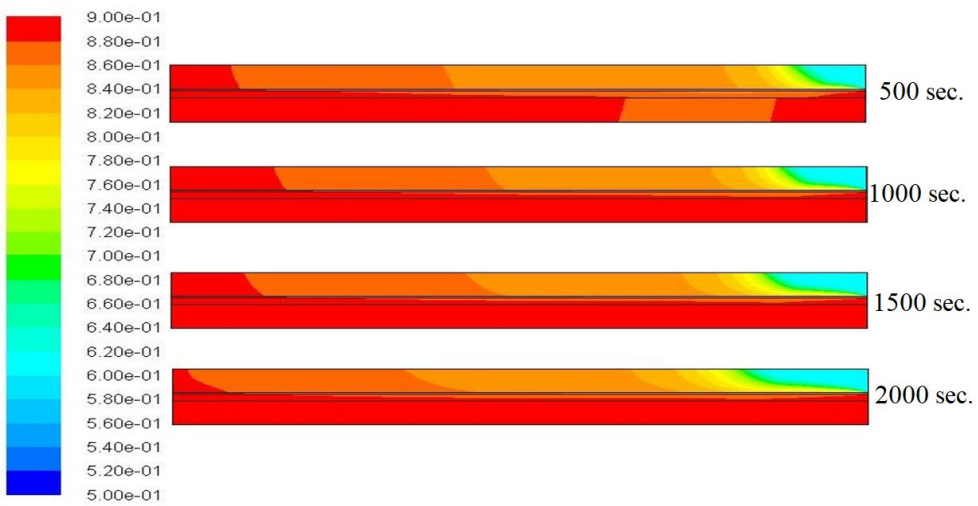

Figure 9.
Particulate matter depositions at different time in diesel fuel case.

Edelweiss Applied Science and Technology
ISSN: 2576-8484
Vol. 8, No. 5: 578-597, 2024
DOI: 10.55214/25768484.v8i5.1719

Figure 10 shows the contours of Particulate matter concentration for Algae B20 blend fuel for different time. It is clearly seen that; the Particulate matter deposition is increased with increase in time. At t = 500 sec, the Particulate matter concentration was little higher at the end of corner. The Particulate matter concentration for the different fuels at t =2000 sec. is shown in figure 11. As explained in figure 7, the maximum Particulate matter concentration found in case of diesel fuel, which also reflect in figure 11. The red color concentration explains the maximum Particulate matter concentration. The addition of the Algae bio-diesel in diesel fuel can help to reduce the emission. The B60 blend was found to be less exhaust emission with less Particulate matter concentration. Normally the PM is proportional to oxygen content available in fuel. Usually, a biodiesel blends have a higher mean molecular weight and the oxygen content than conventional diesel, so any unburnt fuel is more likely to condense as the exhaust cools [25, 26].

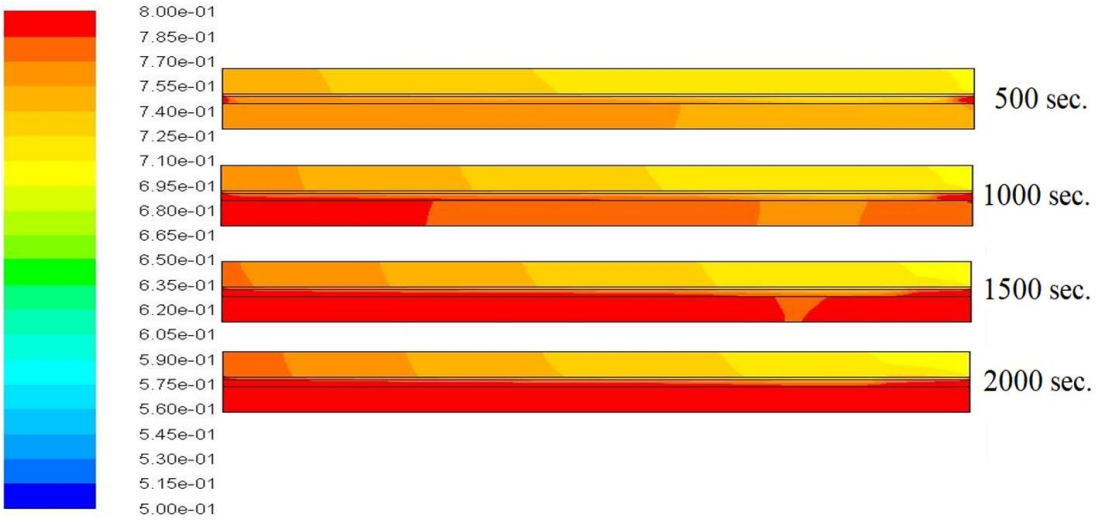

Figure 10.
Particulate matter deposition at different time in B20 algae biodiesel blend fuel case.

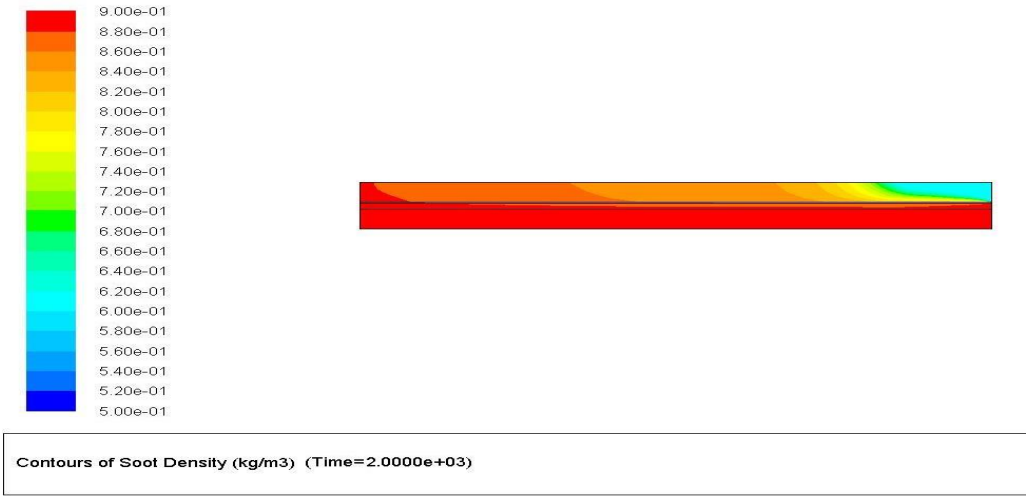

Diesel *(t=2000 sec)*

Edelweiss Applied Science and Technology
ISSN: 2576-8484
Vol. 8, No. 5: 578-597, 2024
DOI: 10.55214/25768484.v8i5.1719

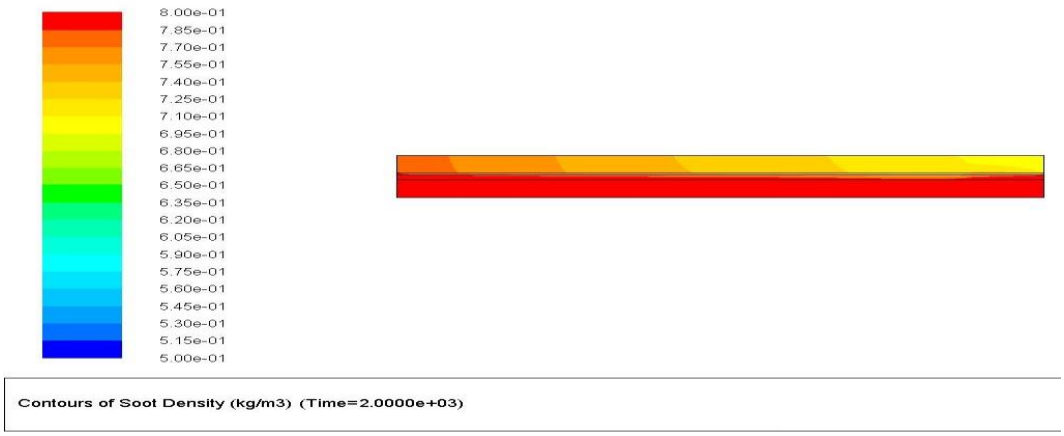

B20 *(t=2000 sec)*

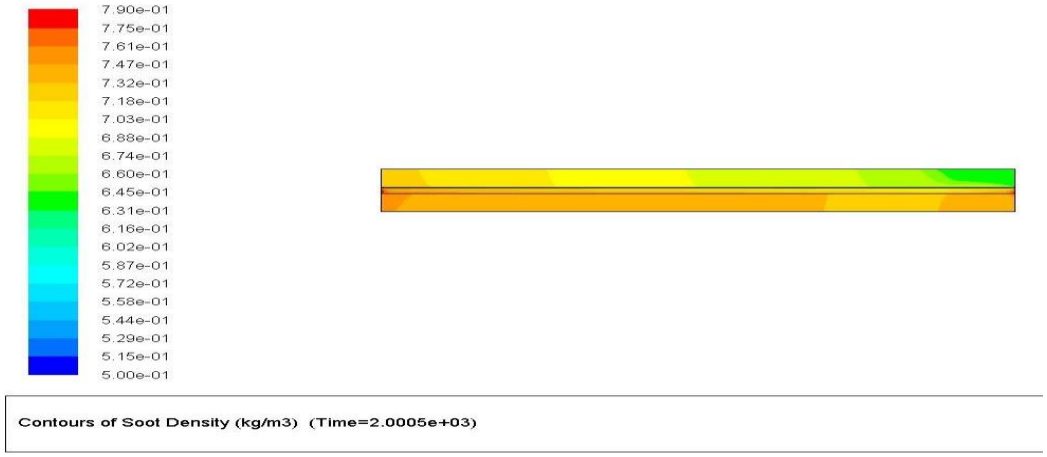

B40 *(t=2000 sec)*

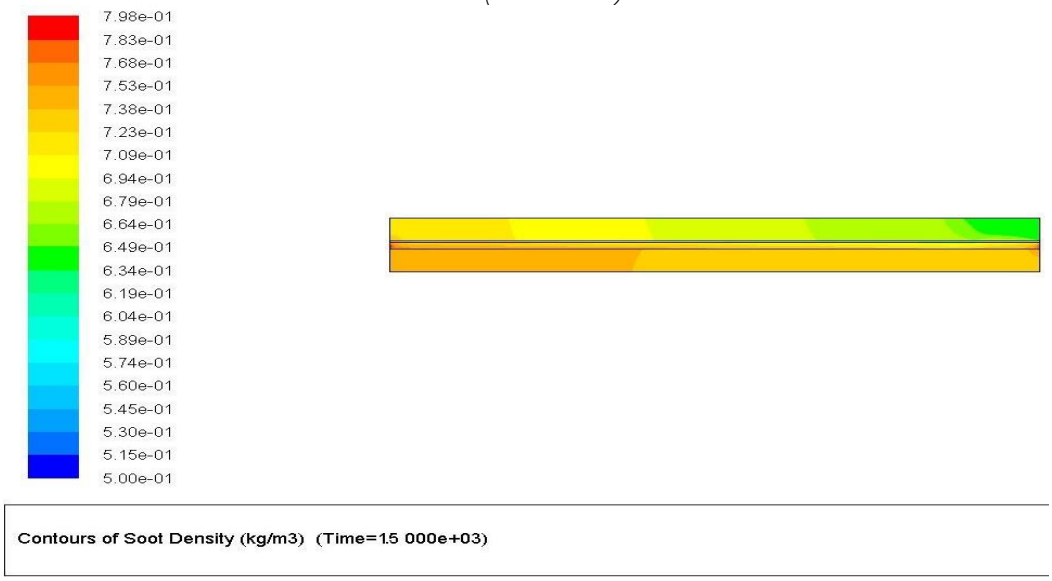

B60 *(t=2000 sec)*

Figure 11.
Particulate matter concentration at t =2000 sec for different fuels.

Edelweiss Applied Science and Technology
ISSN: 2576-8484
Vol. 8, No. 5: 578-597, 2024
DOI: 10.55214/25768484.v8i5.1719

5. Discussion

The experimental and numerical analysis has been done to investigate the effect of different fuel & the following conclusions were drawn from the analysis.The exhaust emission like HC, CO was found lesser with addition of Algae bio-diesel blend in diesel than the pure diesel. The smoke found reduced & NO_x found increased gradually with addition of the Algae bio-diesel.

The Particulate matter concentration rate inside the DPF was seen to be maximum with diesel fuel used. The Particulate matter concentration is increased with increase in time as the Particulate matter particles were deposited on the filter (porous zone). Hence, the pressure drop was increased with increase in Particulate matter concentration. The maximum pressure drop was found with diesel fuel, at obvious due to the maximum Particulate matter deposition in diesel fuel case.

The morphological analysis clears that all the PM samples of all the fuels don't possess any specific shape and are in amorphous structure. The Chemical composition of PM collected from EDS analysis gives important information for the determination of their origin and development processes. SEM–EDS microanalysis clarifies the amount of Oxygen species present in PM composition which is in the order of CI B60 > CI B40 > CI B20 > neat Diesel. The presence of higher amount oxygen may contribute to increment in the reactivity of PM particles & better oxidation properties. Such PM can have better active as well as passive regeneration in DPF leading to reduced backpressure and hence minimizing pressure drop in the Engine performance due to it. So, the potential reactivity of Biodiesel blend PM is more and increases with the increase in Biodiesel content in the fuel due to which DPF performance also seen to be improved.

6. Conclusion

The results showing the reduction in smoke, presence of oxygen in collected soot and reduced rate of clogging in DPF with progressive addition of Algae biodiesel signifies the excellent emission performance of Four stroke Diesel Engine. The Algae Biodiesel blend is proven to be effective for Diesel Engine which needs to be not only compliant with emission control laws but also to have the better performance features like reduced rate of clogging and regeneration dependencies and relevant performance implications of DPF.

Acknowledgment

All authors contributed to the study conception and design. Material preparation, data collection and analysis were performed by Mr. Jayant Nalawade and Dr. R. Prakash. The first draft of the manuscript was written by Mr. Jayant Nalawade and both authors read and approved the final manuscript.

Nomenclature

DPF	Diesel particulate matter
RPM	Rotation per minute
CO	Carbon monoxide
CO_2	Carbon dioxide
NOx	Oxides of nitrogen
NO	Nitric oxide
PM	Particulate matter
VOC	Volatile organic compounds
MPF	Multi-Zone Particulate Filter
PPM	Parts per million
CH_3OH	Methanol
KOH	Potassium hydroxide
BHP	Brake horse power
NDIR	non dispersive infrared

Edelweiss Applied Science and Technology
ISSN: 2576-8484
Vol. 8, No. 5: 578-597, 2024
DOI: 10.55214/25768484.v8i5.1719

CFD	Computational fluid dynamics
SOF	Soluble organic fraction

References
[1] Z. Meng, C. Chen, J. Li, J. Fang, J. Tan, *et al.*, "Particle emission characteristics of DPF regeneration from DPF regeneration bench and diesel engine bench measurements," *Fuel*, vol. 262, p. 116589, 2020.
[2] Z. Zhang, J. E., Y. Deng, M. Pham, W. Zuo, *et al.*, "Effects of fatty acid methyl esters proportion on combustion and emission characteristics of a biodiesel-fueled marine diesel engine," *Energy Conversion and Management*, vol. 159, pp. 244-253, 2018.
[3] J. E., L. Xie, Q. Zuo, and G. Zhang, "Effect analysis on regeneration speed of continuous regeneration-diesel particulate filter based on NO2-assisted regeneration," *Atmospheric Pollution Research*, vol. 7, no. 1, pp. 9-17, 2016.
[4] B. Guan, R. Zhan, H. Lin, and Z. Huang, "Review of the state-of-the-art of exhaust particulate filter technology in internal combustion engines," *Journal of Environmental Management*, vol. 154, pp. 225-258, 2015.
[5] S. Kumar, R. Prakash, S. Murugan, and R. K. Singh, "Performance and emission analysis of blends of waste plastic oil obtained by catalytic pyrolysis of waste HDPE with diesel in a CI engine," *Energy Conversion and Management*, vol. 74, pp. 323-331, 2013.
[6] H. Wang, Y. Ge, J. Tan, L. Hao, L. Wu, *et al.*, "Ash deposited in diesel particulate filter: a review," *Energy Sources, Part A: Recovery, Utilization, and Environmental Effects*, vol. 41, no. 18, pp. 2184-2193, 2019.
[7] Y. Wang, H. Liu, and C. F. F. Lee, "Particulate matter emission characteristics of diesel engines with biodiesel or biodiesel blending: A review," *Renewable and Sustainable Energy Reviews*, vol. 64, pp. 569-581, 2016.
[8] B. L. Salvi, K. A. Subramanian, and N. L. Panwar, "Alternative fuels for transportation vehicles: a technical review," *Renewable and Sustainable Energy Reviews*, vol. 25, pp. 404-419, 2013.
[9] A. Williams, R. L. McCormick, R. R. Hayes, J. Ireland, and H. L. Fang, "Effect of biodiesel blends on diesel particulate filter performance," *SAE Transactions*, pp. 563-573, 2006.
[10] X. Wang, C. S. Cheung, Y. Di, and Z. Huang, "Diesel engine gaseous and particle emissions fueled with diesel–oxygenate blends," *Fuel*, vol. 94, pp. 317-323, 2012.
[11] J. Zheng, J. Wang, Z. Zhao, D. Wang, and Z. Huang, "Effect of equivalence ratio on combustion and emissions of a dual-fuel natural gas engine ignited with diesel," *Applied Thermal Engineering*, vol. 146, pp. 738-751, 2019.
[12] J. Rodríguez-Fernández, J. J. Hernández, and J. Sánchez-Valdepeñas, "Effect of oxygenated and paraffinic alternative diesel fuels on soot reactivity and implications on DPF regeneration," *Fuel*, vol. 185, pp. 460-467, 2016.
[13] A. Obuchi, J. Uchisawa, A. Ohi, T. Nanba, and N. Nakayama, "A catalytic diesel particulate filter with a heat recovery function," *Topics in Catalysis*, vol. 42, no. 1, pp. 267-271, 2007.
[14] V. Di Sarli and A. Di Benedetto, "Modeling and simulation of soot combustion dynamics in a catalytic diesel particulate filter," *Chemical Engineering Science*, vol. 137, pp. 69-78, 2015.
[15] K. Tsuneyoshi and K. Yamamoto, "A study on the cell structure and the performances of wall-flow diesel particulate filter," *Energy*, vol. 48, no. 1, pp. 492-499, 2012.
[16] J. Fang, Z. Meng, J. Li, Y. Du, Y. Qin, *et al.*, "The effect of operating parameters on regeneration characteristics and particulate emission characteristics of diesel particulate filters," *Applied Thermal Engineering*, vol. 148, pp. 860-867, 2019.
[17] G. Wu, A. V. Kuznetsov, and W. J. Jasper, "Distribution characteristics of exhaust gases and soot particles in a wall-flow ceramics filter," *Journal of Aerosol Science*, vol. 42, no. 7, pp. 447-461, 2011.
[18] J. Gong, M. L. Stewart, A. Zelenyuk, A. Strzelec, S. Viswanathan, *et al.*, "Importance of filter's microstructure in dynamic filtration modeling of gasoline particulate filters (GPFs): Inhomogeneous porosity and pore size distribution," *Chemical Engineering Journal*, vol. 338, pp. 15-26, 2018.
[19] K. Yamamoto, S. Oohori, H. Yamashita, and S. Daido, "Simulation on soot deposition and combustion in diesel particulate filter," *Proceedings of the Combustion Institute*, vol. 32, no. 2, pp. 1965-1972, 2009.
[20] K. Yamamoto and S. Ohori, "Simulations on flow and soot deposition in diesel particulate filters," *International Journal of Engine Research*, vol. 14, no. 4, pp. 333-340, 2013.
[21] S. Bensaid, D. L. Marchisio, N. Russo, and D. Fino, "Experimental investigation of soot deposition in diesel particulate filters," *Catalysis Today*, vol. 147, pp. S295-S300, 2009.
[22] B. S. Mahadevan, J. H. Johnson, and M. Shahbakhti, "Experimental and simulation analysis of temperature and particulate matter distribution for a catalyzed diesel particulate filter," *Emission Control Science and Technology*, vol. 1, no. 4, pp. 255-283, 2015.

[23] A. Suresh, A. Khan, and J. H. Johnson, "An experimental and modeling study of cordierite traps-pressure drop and permeability of clean and particulate loaded traps," *SAE Transactions*, pp. 245-264, 2000.
[24] M. K. Khair, "A review of diesel particulate filter technologies," *SAE Technical Paper*, no. 2003-01-2303, 2003.
[25] V. H. Nguyen and P. X. Pham, "Biodiesels: Oxidizing enhancers to improve CI engine performance and emission quality," *Fuel*, vol. 154, pp. 293-300, 2015.
[26] J. Song, M. Alam, A. L. Boehman, and U. Kim, "Examination of the oxidation behavior of biodiesel soot," Combustion and Flame, vol. 146, no. 4, pp. 589-604, 2006.

Edelweiss Applied Science and Technology
ISSN: 2576-8484
Vol. 8, No. 5: 578-597, 2024
DOI: 10.55214/25768484.v8i5.1719